Applied Chemistry Today **19(73)** (2024) 177-198

Semnan University

Applied Chemistry Today

Journal homepage: https://chemistry.semnan.ac.ir/

ISSN: 2981-2437

Research Article

Selective Determination of Polycyclic Aromatic Hydrocarbons in Water, Wastewater, Vegetables and Soil after HS-SPME Using Molecularly Imprinted Polymer/UMCM-1/ Deep Eutectic Solvent Fiber by GC-FID

Roya Mirzajani*, Marzyeh Dianati

Department of Chemistry, College of Science, Shahid Chamran University of Ahvaz, Ahvaz, Iran

PAPER INFO

Article history:
Received: 26/Jun/2024
Revised: 25/Sep/2024
Accepted: 08/Nov/2024

Keywords:
PAHs,
Headspace
solid- phase microextraction,
Metal–organic frameworks,
Deep eutectic solvents,
Molecularly imprinted polymer,
GC-FID.

ABSTRACT

In this study, a solid-phase microextraction (SPME) fiber based on metal-organic frameworks/deep eutectic solvents/molecularly imprinted polymers (MOF-DES/MIPs) was developed for the rapid and efficient extraction of polycyclic aromatic hydrocarbons (PAHs) from soil, vegetables, water, and wastewater samples, followed by gas chromatography-flame ionization detection. The quality and porosity of the MOF-DES/MIPs fiber were evaluated using scanning electron microscopy (SEM) and BET surface area analysis. The effects of key parameters on extraction efficiency and precision were investigated and optimized using a Box-Behnken design. Under optimized conditions, the developed method exhibited linearity over a calibration range of 0.05-150 µg L^{-1}. The detection limits and relative standard deviations (RSD) (n=5) ranged from 0.015 to 0.019 µg L^{-1} and 2.0% to 4.9%, respectively. Individual PAH recoveries from spiked real samples were between 94.3% and 106.1%. The method's high extraction efficiency, use of safe and inexpensive components, short analysis time, and simplicity suggest it has significant potential for the selective determination of trace PAHs in various real samples, including water, vegetables, and surface soils from oil exploration areas.

DOI: https://doi.org/10.22075/chem.2024.34571.2282

* **.corresponding author:** Associate Professor of Analytical Chemistry. *E-mail address: rmirzajani@scu.ac.ir*

How to cite this article: Mirzajani, R., & Dianati, M. (2024). Selective Determination of Polycyclic Aromatic Hydrocarbons in Water, Wastewater, Vegetables and Soil after HS-SPME Using Molecularly Imprinted Polymer/UMCM-1/Deep Eutectic Solvent Fiber by GC-FID. *Applied Chemistry Today*. **19(73)**, 177-198. (in Persian)

1. Introduction

Polycyclic aromatic hydrocarbons (PAHs) are a diverse group of organic compounds characterized by the presence of two or more aromatic rings without heteroatoms. As some of the most hazardous persistent organic pollutants (POPs), PAHs pose risks to both environmental and public health and are included in the priority pollutant lists of the US Environmental Protection Agency (US EPA) and the European Union (EU). Their persistence, bioaccumulation, genotoxicity, mutagenicity, human carcinogenicity, and teratogenic properties, combined with the availability of instrumentation and standards for detecting them at low concentrations, underscore their significance as contaminants. PAHs are primarily generated through industrial activities, such as fossil fuel processing, oil refining, petrochemical production, and other anthropogenic processes like coal processing, vehicle emissions, packaging, drying, roasting, cooking, and food processing. They also arise from natural sources, including forest fires, biological and microbial activity, and volcanic eruptions.

Once released, PAHs can disperse throughout various environmental media, such as water, air, sediments, plants, and soil, leading to contamination of terrestrial and aquatic species. Consequently, elevated levels of PAHs can be found in the human food supply. Estimates suggest that the absorption of PAHs through the consumption of vegetables and fruits — accounting for approximately 31% of total food intake — averages between 5% and 10% [1]. However, daily PAH intake from these food sources can vary significantly based on individual dietary preferences, as well as environmental factors, product storage conditions, and food processing methods. Thus, vegetables and fruits represent a vital focus for PAH studies. Additionally, oil exploration activities contribute to the release of PAHs into the soil, water, and air, exposing individuals living near petroleum facilities to contaminated resources. [2].

The high hydrophobic properties and low solubility of PAHs in water and their lipophilic properties, the possibility of easily passing through lipid membranes, lead to their accumulation in aquatic organisms and interfere with the normal function of DNA, their active absorption in soil and sediments, and as a result, their biological effectiveness [3-5]. Therefore, it is crucial to monitor their environmental exposure and develop efficient, sensitive and selective methods for their removal in industrial wastewater samples containing a low concentration of them with a very complex matrix.

Correspondingly, sample preparation, especially involving extraction, often required prior to their analysis and occupies a strategic place. Various analytical methodologies have been developed to extraction, determination and analyze PAHs. Among the different Sample preparation techniques, Solid-phase microextraction (SPME), is a useful sample pretreatment technique, in which sampling and sample preparation are integrated into one step and benefit from advantages such as high speed, pre-concentration and field-compatible. This method is performed by using a polymer thin-film coating on a capillary fiber or a composite that comes in the form of fiber that is exposed to a gaseous or liquid sample or the space above a liquid or solid sample [4, 6-10].

Recently, due to lack of selectivity and fragility of commercially available fibers new supports, coating materials and fiber composites were developed. Considering that the nature of the targeted analytes and the properties of the absorbent coated on the fiber determines the extraction performance of SPME, new materials with surface topography and special internal pore structure to increase sensitivity, reproducibility, selectivity, thermal and chemical

stability, have been made. Carbon materials (multiwall carbon nanotube and graphene), metal nanoparticles and nanorods (Au nanoparticles and ZnO nanorods), silicate, ionic liquids (ILs), Metal-organic frameworks (MOFs) and deep eutectic solvents (DESs), these are examples of materials that have been successfully explored directly or indirectly as fiber materials in sample pretreatment [3,11-15].

Metal-organic frameworks (MOFs) are composed of organic bridging ligands and metal ion building units, which interact through coordination bonds. MOFs are more versatile and advantageous compared to other sorbents and have received increasing attention because of their large surface areas, diverse structures, tailorable molecular properties, tunable porosity, nanoscale cavities, good thermal stabilities and ease of functionalization. Many researches indicated that in the adsorption mechanism with the organic linkers of MOFs and hydrophobic organic compounds (e.g., PAHs, PCBs), which are hydrophobic interactions and π- stacking, nano/micropore sizes and large surface areas also have an important role. Despite their many advantages, many of them have significant drawbacks such as low water, and light resistance, poor electrical conductivity, mechanical strength and also susceptibility to slow degradation. One of the possible and an effective approach to improve the properties of the MOFs is to preparation of their hybrid nanocomposite or functionalize them hybrid with other materials such as graphene, carbon nanotube, Nanoparticles and extractive solvents (ionic liquids, deep eutectics, etc.) [11, 16].

Recently, extensive receptors showed that Molecularly imprinted polymers (MIPs) can be used as sorbents due to thermal, mechanical, and chemical constancy their easy preparation and highly selective recognition capabilities [17-20]. DES-based MIPs have superior adsorption capacity and selectivity compared to MIPs made without the DESs. Because, DESs increase the availability of important functional groups on the surface of MIPs which improves their binding affinity and selectivity [21, 22]. In addition, DESs can act as auxiliary solvents spreading over the surface of the resulting polymer, promoting the functional solvents to form specific binding sites and produce more rigid MIPs without shrinking or swelling which can improve their affinity and selectivity [23, 24]. Also, the combination of MIPs and Deep Eutectic Solvents (DESs) (as substrates) with MOFs in SPME technique, in addition to resolve the drawbacks of MOFs, enhances the selectivity, efficiency and performance of the extraction process [9, 25]. MIP is not only used in combination with the MOFs in SPME, but also shows an interesting function as an adsorbent alone [26].

To prepare MIPs, covalent or non-covalent bondings are formed between monomers and template. In the next step, a cross-linking agent is added to form a three-dimensional polymer network, and finally, the template can be removed by chemical reaction or extraction. Due to the agreement of the microcavities in terms of dimensions, shape and size with the template molecule, the resulting MIP has an excellent ability to recognize template molecules and specifically absorb them [6, 9, 26].

DES are green solvents that have been used in the last few years as an alternative to ionic liquids (ILs) as an extraction medium due to their low toxicity, simple synthesis and low cost. According to the definition, a DES generally consists of two or three hydrogen bond donor (HBD) and hydrogen bond acceptor (HBA) components, which are non-toxic. The melting point of the resulting DES is lower than each of the two components. One of the widely used HBDs due to its an inexpensive, nontoxicity, and biodegradability is the quaternary ammonium salt of choline chloride (ChCl), which interacts with

hydrogen bond donors (HBDs), such as carboxylic acids (e.g. , oxalic acid), polyols (e.g., glycerol), or urea and rapidly forms a high-purity liquid. The resulting DES does not react with water, which allows for easy storage. Also, they are biocompatible, biodegradable, non-toxic inexpensive and non-flammable. These advantages have caused DES to be widely applied in various fields, including organic synthesis, catalysis, electrochemistry, solubility studies and SPME [3-5, 9, 27].

Therefore, based on the reported works and considering the benefits of MOFs, in this case, the UMCM-1 was used as a fiber skeleton to prepare the fiber. In order to improve the performance of the fiber, molecular imprinted polymer (MIP) and deep eutectic solvents (DESs) (as substrate solvent) were used to make the composite, which can significantly increase the performance of UMCM-1. PAHs extraction was carried out using MOF-DES/MIPs fiber-SPME and analyte detection were achieved by GC-FID detection.

2. Experimental

2.1. Chemicals and reagents

All chemicals were of the highest available purity and doubled distilled water was used throughout. PAHs containing, 1-naphthol, 2-naphthol, anthracene, 1,10-phenantherene with the purity >99% were purchased from Merck (Darmstadt, Germany, www.merck.com). Methacrylic acid (MAA), ethylene glycoldimethacrylate (EGDME) and azo (bis)-isobutyronitrile (AIBN) were supplied from Sigma Aldrich (St. Louis, MO, USA). Zn $(NO_3)_3$ 6H2O, benzene-1,4-dicarboxylic acid (DBC), benzene-1,3,5-tricarboxylic acid (BTC) provided from Sigma Aldrich (https://www.sigmaaldrich.com, USA). Choline chloride and glycerol were supplied form Merck and used for synthesis of deep eutectic solvent (DES). All organic solvents (Acetonitrile, ethanol, toluene, N,N-dimethylformamide (DMF), methanol, acetone, n-hexane) and water of HPLC grade were purchased from Merck. Other reagents were of analytical grade and doubly distilled water was used in all experiments. Standard stock solutions containing a 100 mg L^{-1} concentration of PAHs compounds were prepared by dissolved in methanol. All stock solutions were stored in dark glass bottles at 4 ˚C. Working standard solutions were prepared daily from their stock standard solutions.

2.2. Apparatus

A Gas chromatograph (model CP-3800, Varian, Germany) was used in the investigations and quantitatively determination of PAHs. The GC equipped with a BP21 capillary column (25 m×0.32 mm I.D, film thickness 0.5 μM) and a flame-ionization detector (GC-FID). The temperatures of the initial oven temperature were programmed from 80 ˚C (for 1 min) to 200 ˚C at a rate of 10 ˚C min^{-1} then increased to 260 ˚C at a rate of 20 ˚C min^{-1}. Also, the temperature of injection port was set at 280 ˚C. The FID temperature was held at 300 ˚C. The carrier gas was high-purity nitrogen (99.999%) with the flow rate of 1 mL min^{-1}. Functional groups of MOF- DES/MIPs nanocomposite were identified using a FT-IR spectrometer (Spectrum two, Perkin Elmer Inc.).

X-ray diffraction (XRD) data were obtained by Auto MATE II (Rigaku corp. Japan). Brunauer– Emmett–Teller (BET) analyses were carried out using apparatus BellSORP- miniII (Bell Japan Inc.). The morphology of the nanocomposite and monolithic fiber were observed by a scanning electron microscopy (SEM, LEO 1455VP). The stirring was carried out by MR Hei-standard Heidolph magnetic stirrer (Germany).

2.3. Synthesis of UMCM-1 MOF

The UMCM-1 MOF was synthesized according to the previously reported method [9]. Briefly, first,

0.656 g of Zn $(NO_3)_2$ $6H_2O$, 0.104 g of H_2BDC and 0.233 g of H_3BTC were dissolved in 20 mL of DMF solvent. The resulting mixture was ultrasonicated for 10 minutes, next was transferred to a Teflon-lined stainless steel autoclave , then the autoclave was heated at 85°C for 3 days. The product was immersed in $CHCl_3$ solvent for 72 h, during that, the activation solvent was poured out and was replaced three times with fresh solvent. Then, it was dried at room temperature.

2.4. Preparation of DESs

The three major groups of HBDs that widely used in combination with ChCl for the synthesis of DESs are: carboxylic acids, amides and alcohols [28, 29]. The reported works indicated that ChCl-glycerol DES systems have more ability to absorbent ion or extraction the analytes from their complex matrices than other common eutectic solvents [30-33]. Therefore, in this work, the eutectic mixtures of ChCl-glycerol were prepared at molar ratio of 2:1 and utilized as an extraction medium for the extraction of the PAHs from the different samples. DES was prepared by mixing glycerol as hydrogen bond donor and choline chloride salt as a hydrogen bonding acceptor at molar ratio of 2:1. The mixture was constantly stirred at 90 ◦C. After 50 min, the eutectic homogeneous transparent liquid was formed.

2.5. Preparation of MOF- DES/MIPs fiber

To synthesize the MIPs part from MOF- DES/MIPs monolithic fiber, four components, anthracene molecules as a template, MAA as a functional monomer, EGDMA as a cross-linking agent and AIBN as an initiator of the imprinting polymerization were used. To prepare this monolithic fiber, 90.0 mg of metal-organic framework (UMCM-1) from the previous step, was added in 10 mL of DMF solvent under ultrasound waves. After 20 min, first 15 mL acetonitrile containing 5.0 mM of the anthracene, then 50.0 mM of MAA with 100 μL of DES were added to the desired solution and stirred for 1 h. Subsequently, 500.0 mM of EGDME and 0.5 mM of AIBN were added to the solution then sonicated for 20 min. In the following, 2 mL of repolymerization solution was poured into a small glass tube and was deoxygenized using nitrogen gas for 5 min. To form the MOF-DES/MIPs monolithic fiber, capillary tubes with a length of 7.5 cm and a diameter of 1.2 mm, were inserted into a small glass tube containing pre polymerization mixture, previously degassed with a N_2 stream for 5 min and afterwards, filled tubes were introduced in an oven and polymerization took place at 60 °C for 12 h. Eventually, the capillary tube was removed from polymeric fiber. To remove the template molecules, MOF-DES/MIPs were washed and sonicated separately for 30 min with (30 mL) toluene. The discarded supernatant was replaced with the same amount of fresh toluene solution. The washing steps mentioned above were repeated five times, until no traces of anthracene molecules were detected in the discarded supernatant by using of GC- FID analysis. The non-imprinted polymer particles (NIP), were prepared under the same conditions, but without the addition of the anthracene as a template.

2.6. Analytical procedures

The head space solid phase microextraction (HS-SPME) was performed using a 10 mL sample vial containing 5 mL of analyte standard solution (including anthracene, phenanthrene, 1-naphtol and 2-naphtol). Then, the fiber housed in the needle of a 5 mL homemade SPME syringe was suspended above the sample solution. The vial size, sample

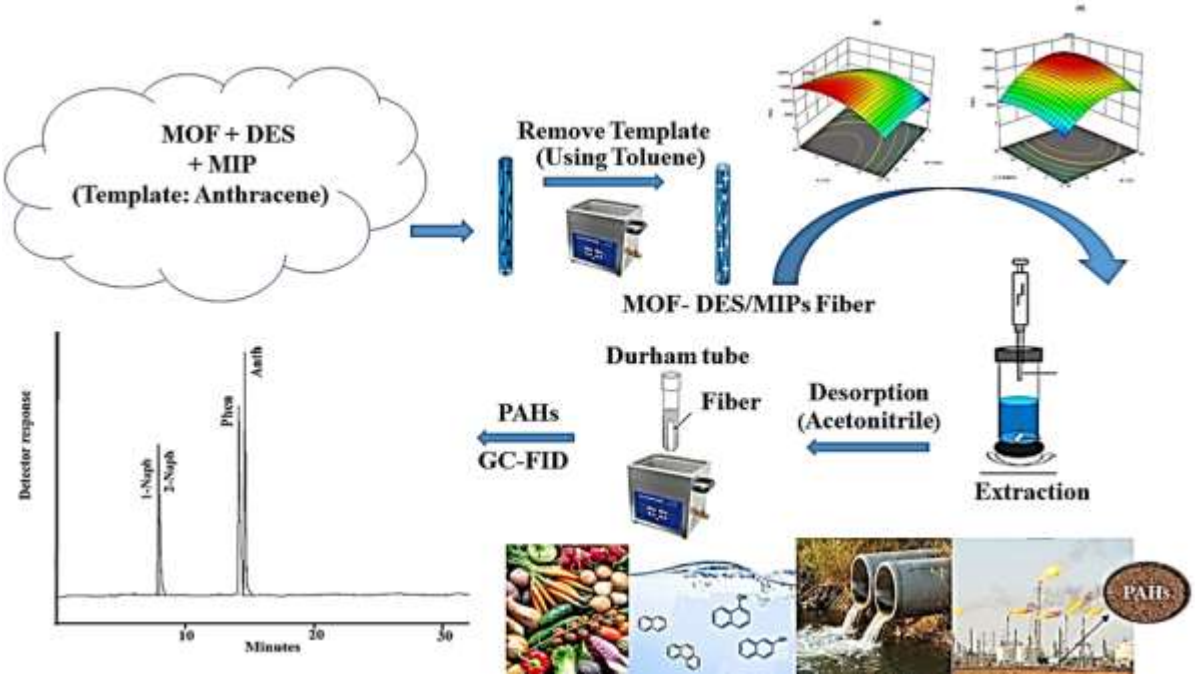

Fig. 1. Schematic design of the fiber preparation steps and the microextraction method steps.

The vial size, sample volume and headspace volume was kept constant in each experiment. Also, it is important to place the fiber at the same depth in the headspace every time to improve reproducibility. After the addition of sodium chloride and magnetic stirring bar, the vial was tightly closed with a teflon-coated septum to prevent sample loss due to evaporation. To obtain good precision must be used a constant temperature for all extractions. Therefore, the sample vials were heated by using a hot plate accommodated in a glass beaker contained some water and a thermometer was placed in it. After extraction, to desorb the analytes, the fiber was removed from the vial and immersed in a durham tube containing 0.5 mL of acetonitrile (as the desorption solvent). The tube was sealed and sonicated for 10 minutes at 25°C. Then the final solution was used for Analysis with GC-FID device. Sample volume and extraction space were kept constant in each experiment. The schematic design of the fiber preparation steps and the microextraction method used is shown in Fig. 1.

2.7. Real samples

River water, tap water and wastewater samples were collected from the Karun River (Ahvaz, Iran), our laboratory (Shahid Chamran university of Ahvaz, Iran) and Ahvaz city sewage respectively. Ground drainage water samples were obtained from Omidiyeh, Iran. The samples were filtered through a Whatman No. 45 filter paper. All water samples were stored in amber glass bottles at 4°C in darkness before use. All vegetable samples (lettuce, carrot, radish, potato, cucumber) were bought from local supermarkets in Ahvaz (Iran). About 200.0 g of each vegetable samples were thoroughly homogenized using a juice extractor and juice were centrifuged at 4000 rpm for 5 min. the Samples were then filtered using a Whatman No. 45 filter paper and packed in amber glass bottles and stored at 4 °C in the dark until analysis. To extract the analyte from the sample matrices, 1.0 g juice samples in 5 mL double distilled water were transferred into 10 mL vials and the PAHs was extracted from the solution using HS-SPME according to the proposed method. The surface soil samples were collected from the side of oil field near the city of Omidiyeh in Iran.

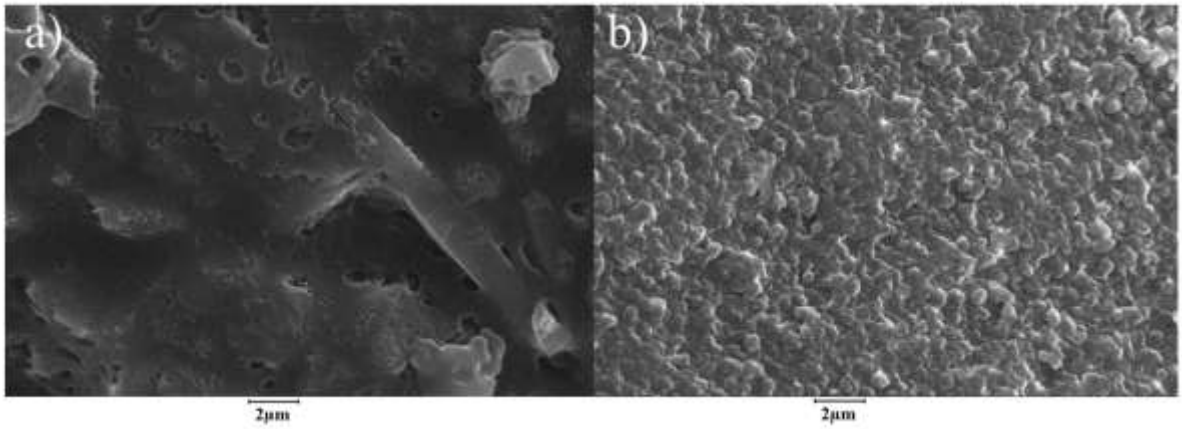

Fig. 2. SEM image of a) UMCM-1, b) UMCM-1-DES/MIP fiber.

PAHs were extracted from soil samples according to the previously reported procedure [34]. For this purpose, 2.0 g of soil was added to 10 mL n-hexane and acetone (1:1) and was sonicated for 30 min. The mixture was centrifuged at 4000 rpm for 10 min to separate the soil from the solution. Then, the solution was passed through the filter paper to remove any solid residue. The resulted solution was stored in a dark clean container. The extraction was repeated five times on each soil and the resulting supernatant was added to the previous extract. The solvent volume of the extract was reduced to 2 mL by passing nitrogen gas through the solution for about 30 min. Finally, 100 μL of the concentrated extract was added to 5 mL distilled water and the HS-SPME procedure was applied according to the proposed method.

3. Results and discussion

3.1. Characterization of DES, UMCM-1 and MOF- DES/MIPs

SEM images of UMCM-1 and UMCM-1-DES/MIP fibers are shown in Fig. 2. Based on these figures, UMCM-1 showed a crystalline structure with relatively uniform size. After exiting the template, UMCM-1-DES/MIP fiber surface became porous; this issue can be clearly seen in the Fig. 2. In addition to the important factors of π-π stacking interactions and the hydrophobic adsorption of PAHs on MOF [35], this porosity of the UMCM-1-DES/MIP fiber surface, which forms specific absorption sites, can have a significant impact on the absorption process of PAHs.

In order to ensure preparation of DESs and elucidate the interactions between the two components (glycerol and choline chloride) resulting in the formation of DES, FT-IR spectra were recorded. Fig. 3 shows a comparison of the FT-IR spectra of the pure components and the DES formed. Considering that the formation of hydrogen bonds between HBA and HBD leads to the synthesis of deep eutectic solvents, therefore the structure of reactants has a great influence on the location of the bonds. In FT-IR spectra, the stretching vibrations of OH glycerol (hydrogen bonding donor) and choline chloride (hydrogen bonding acceptor) peaks appeared in the region of 3000-3500 cm^{-1} [9]. Vibrations in the regions of 2969 cm^{-1} and 1063 cm^{-1}, were attributed to vibrations of C-H and N-H present in choline chloride [9] which appears with a slight shift towards a higher wave number in the spectrum related to the Des solvent. This shift indicates the formation of new hydrogen bonds between the components and as a result the successful formation of Des solvent.

In infrared spectroscopy of UMCM-1 in Fig. 4, absorption peaks of aromatic C=C stretching (1558 cm^{-1}), bending vibration of O-C-O (1386 and 1627 cm^{-1}), vibration of O-H (3450 cm^{-1}) and bending vibration of C-H (760 cm^{-1}) belonged to

BTC and BDC existing in the structure of UMCM-1.

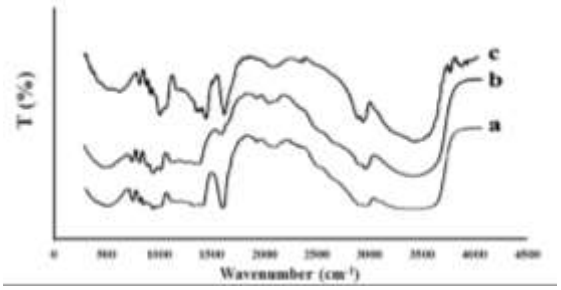

Fig. 3. FTIR spectra of a) Choline chloride, b) Glycerol, c) Deep eutectic solvent (DES).

For poly (MAA-EGDMA)–based polymer, four strong infrared absorption bands of hydroxyl groups (3650 cm^{-1}), methyl groups (2955 cm^{-1}), carbonyl groups (1735 cm^{-1}), and methyl groups (1458 cm^{-1}) were observed. Other absorption bands groups such as stretching vibrations of C-O were found in 1162 and 1261 cm^{-1} region. The MOF-DES/MIPs nanocomposite has similar infrared spectrum as shown in Fig. 4. But alteration in intensity of several absorption regions were observed. The increase in the intensity of absorption peaks in infrared spectrum of a metal-organic framework-deep eutectic solvents / polymer was observed in regions of 760 and 1386 cm^{-1} Compared to UMCM-1 spectrum. The peak related to aromatic C=C stretching (1558 cm^{-1}) cannot be seen due to overlapping, as well as, an increase in the absorption peak in the regions of 2955 (CH_2), 1458 (CH_2) and 1735 cm^{-1} (C=O) in infrared spectrum of a MOF-DES/MIPs. Also, an increase in the absorption peak in the regions of 1162, 1261 and 956 Cm^{-1} (C-O, C-OH, N-C-C bending), confirmed successful participation of DES solution and polymer in MOF-DES/MIPs nanocomposite synthesis.

The X-ray diffraction (PXRD) spectrum of the crystal structure corresponding to UMCM-1 and UMCM-1-DES/MIP Nanocomposite is be shown in Fig. 5. Accordingly, the characteristic peaks in the region of 2Θ=12 are attributed to the UMCM-1 structure, which is consistent with the previously

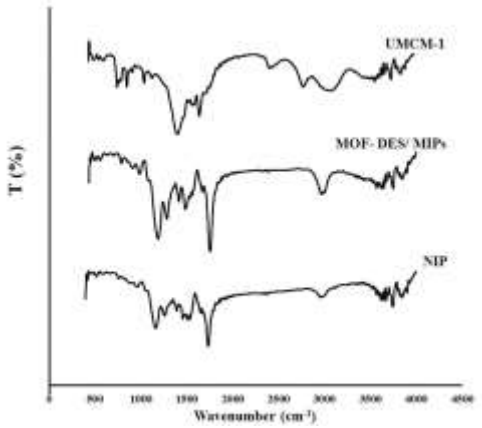

Fig. 4. FTIR spectra of synthesized UMCM-1, MIP and NIP.

reported works [36]. XRD analysis of UMCM-1-DES/MIP indicates the MOF presence in the polymer matrix. Also, it could be clearly seen that; the UMCM-1 maintains its crystallinity even in the UMCM-1-DES/MIP nanocomposite with its characteristic peaks. This profile indicates that the adding DES and polymer to UMCM-1 did not affect its crystalline properties. This good compatibility between UMCM-1, DES and polymer, prevents the leakage and appearance of free standing UMCM-1 particles during application and as a result this enhances the stability of the fiber.

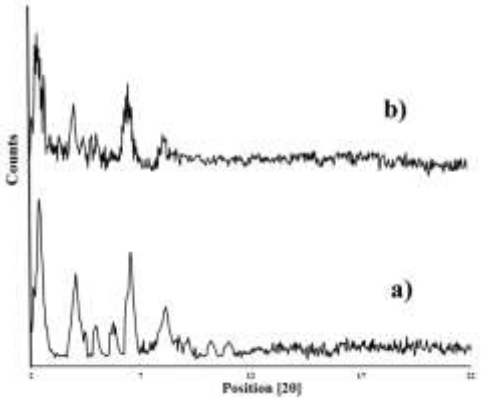

Fig. 5. XRD pattern of a) UMCM-1and b) UMCM-1-DES/MIP fiber.

The pore volume and surface area of the synthesized were determined by the BET technique. The summary data for the BET plot of the UMCM-1-DES/MIP fiber is be shown in table 1. In general, the large cavity volume and the large surface area are advantages for the polymer to easily absorb the template molecule.

The structure and porosity of the particles affect the efficiency of the MIP and cause the template molecule to have easy access to the bonding sites on the surface of the absorbent, and as a result, the detection and extraction of the template molecule is easier, which can increase adsorption capacity. According to BET plot the total specific surface area of 363.6 m^2 g^{-1} was determined for UMCM-1-DES/MIP. This shows that the UMCM- 1-DES/MIP has a high specific absorption to analyte and this is due to combining the favorable attributes of UMCM-1 surfaces and MIP.

Table 1. Results of BET plot for UMCM-1-DES/MIP fiber.

	BET plot	
V_m	83.538	[cm^3(STP) g^{-1}]
$a_{s,BET}$	363.6	[m^2 g^{-1}]
C	75.702	[cm^3 g^{-1}]
Total pore	0.9926	
Mean pore diameter	10.92	[nm]

3.2. Optimization of conditions

3.2.1. *Optimization of desorption conditions*

In order to optimize the parameters affecting the desorption step, parameters such as the type of desorption solvent and desorption time were optimized using one variable at a time. Different organic solvent including methanol, acetonitrile, acetone and combination of methanol: acetone, methanol: acetonitrile, acetone: acetonitrile mixtures were used for PAHs desorption. As shown in the Fig. 6, the maximum extraction efficiency was achieved for acetonitrile solvent. Also, based on the optimum time test results, the optimum time for ultrasonic used in desorption step was 10 minutes. The carry-over effects of the system were studied by a second fiber desorption. No peaks were observed at the retention time of the PAHs.

3.2.2. Experimental design and optimization of adsorption parameters by Box– Behnken Design

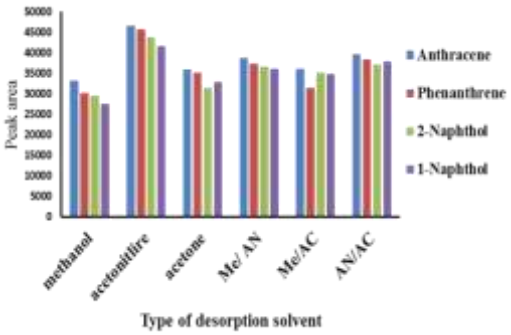

Fig. 6. Effect of type of organic solvent on extraction efficiency of PAHs.

In order to optimize the parameters affective on adsorption step in the PAHs extraction using the Headspace SPME (HS-SPME) technique was performed Box–Behnken design through response surface methodology. A PAH concentration of 10 µg L^{-1} was used in this step. Based on our primary experiments, five variables may affect the experimental response include extraction time (t), initial pH of sample solution, stirring rate (R), amount of salt (S) and extraction temperature (T). Since the primary experiments to investigate the effect of pH by one variable at time method showed that the change in pH does not have a significant effect on the peak area of the PAHs, so the pH of the sample solution was set at neutral point in the continuation of the experiments. This is probably due to the fact PAHs do not have ionizable groups, so they are stable over a wide range of pH [37]. Therefore, in the following, four variables include extraction temperature (40–80 ºC), extraction time (5–30 min) stirring rate (300-800) and amount of salt (%,w/v) (0–20 %, w/v) chosen as the main factors affecting adsorption step. 27 runs BBD experiment was conducted to optimize the extraction conditions shown in Table 2.

The response used as the input data was obtained by calculating the mean of the set of 4 normalized peak areas corresponding to the analytes.

Table 2. The design and results of the BBD experiments.

Run no.	Variables				Mean peak areas
	T(ºC)	t(min)	R (rpm)	S (%W/V)	
1	-	+	0	0	74027
2	-	0	0	0	45687
3	0	0	+	+	111746
4	0	-	0	0	103947
5	0	0	-	-	73719
6	0	0	0	0	135454
7	-	-	0	0	48686
8	0	0	0	0	140455
9	0	+	0	0	120367
10	+	0	0	0	129469
11	0	0	0	0	140657
12	0	0	-	-	125040
13	+	0	-	-	82813
14	0	-	+	+	84612
15	-	0	-	-	50499
16	-	0	0	0	58857
17	0	+	-	-	132914
18	0	0	+	+	94021
19	0	-	-	-	86503
20	+	+	0	0	140191
21	+	0	+	+	114324
22	-	0	+	+	74438
23	0	+	+	+	149693
24	+	0	0	0	76364
25	0	-	0	0	50824
26	+	-	0	0	67035
27	0	+	0	0	161793

By using Design-Expert software (V. 12.0.3.0, Stat-Ease Inc., Minneapolis, MN, USA) on the simulation of experiment data, a second-order polynomial equation was obtained as follows:

$$Y = \beta_0 + \beta_1 A + \beta_2 B + \beta_3 C + \beta_4 D + \beta_{12} AB + \beta_{13} AC + \beta_{14} AD + \beta_{23} BC + \beta_{24} BD + \beta_{34} CD + \beta_{11} A^2 + \beta_{22} B^2 + \beta_{33} C^2 + \beta_{44} D^2 \quad (1)$$

Y: The predicted response by the model, A: code of extraction temperature (- 1, 0, 1), B: code of extraction time (- 1, 0, 1), C: code of salt concentration (- 1, 0, 1), D: Stirring rate (- 1, 0, 1). β_0 is a constant, β_1, β_2, β_3 and β_4 are the calculated linear coefficients of A, B, C and D coefficients as independent variable. β_{12}, β_{13}, β_{14}, β_{23}, β_{24} and β_{34} are interaction coefficients between the factors and, β_{11}, β_{22}, β_{33} and β_{44} are quadratic coefficients of β. The terms (AB, AC, AD, BC, BD, CD) and (A^2, B^2, C^2, D^2) represent the interaction and second-order coefficients of the parameters, respectively. Next, the analysis of variance (ANOVA) technique by Design-Expert software was used for significance analysis of the model above at 95% confidence level. Model F-value of 36.06 and the P value less than 0.0001 shown in Table 3 indicate the model is significant at 95% confidence level.

$$Y = -420762.00 + 21500.17A + 28114.88B + 19155.81C + 6445.52D + 11953.75AB + 9983.69AC + 1893.06AD - 2924.31BC + 4667.44BD - 8398.94CD - 43194.32A^2 - 10919.01B^2 - 19513.79C^2 - 15952.73D^2 \quad (2)$$

Table 3. Analysis of variance (ANOVA) for the experimental result of BBD.

Source	Sum of Square	Df	Mean Square	F-value	p-value
Model	31590000000	14	2256000000	36.06	<0.0001
A-T	5547000000	1	5547000000	88.67	<0.0001
B-t	9485000000	1	9485000000	151.62	<0.0001
C-S	4403000000	1	4403000000	70.39	<0.0001
D-R	498500000	1	498500000	7.97	0.0154
AB	571600000	1	571600000	9.14	0.0106

AC	398700000	1	398700000	6.37	0.0267
AD	14330000	1	14330000	0.2291	0.6408
BC	34210000	1	34210000	0.5468	0.4739
BD	87140000	1	87140000	1.39	0.2608
CD	282200000	1	282200000	4.51	0.0552
A^2	9951000000	1	9951000000	159.06	<0.0001
B^2	635900000	1	635900000	10.16	0.0078
C^2	2031000000	1	2031000000	32.46	<0.0001
D^2	1357000000	1	1357000000	21.70	0.0006
Residual	750700000	12	62560000		
Lack of Fit	733300000	10	73330000	8.44	0.1105
Pure Error	17370000	2	8687000		
Cor Total	32340000000	26			

Comment: R^2 = 0.9768, adjusted R^2 = 0.9497, predicted R^2 = 0.8682, adequate precision = 18.1996.

In addition, the p-values for the lack of fit were greater than 0.05 (0.1105), demonstrating that the effect of the lack of fit for the predicted model was insignificant. In addition, the quality of the fit of the polynomial model equation was explained by the determination coefficient (R^2 = 0.9768). R squared is a measure of the amount of deviation around the mean explained by the model. The large adjusted R^2 values indicate a good relationship between the experimental data and the fitted model and thus the suitability of the model.

The optimal extraction conditions were found to be at a extraction temperature of 68 ºC, extraction time of 28 min, Stirring rate of 580 and salt concentration 10.5% w/v.

3.2.3. Effects of interactive variables

Fig. 7 shows 3D response surface plots that investigate the influence of independent factors on the response variable. These plots depict the interaction of each two variables by keeping the others at their central level for microextraction of PAHs compounds.

Fig. 7 a, b shows the interactions of salt concentration and extraction time with the temperature on the peak area of analytes. Temperature can mainly affect on the extraction of analyte in HS-SPME. By increasing the temperature of the sample solution, the vapor pressure of the analyte is increased. Therefore, the analyte can be existed in headspace of sample and extracted by the SPME fiber. But at higher temperatures, analytes do not tend to be absorbed into the fiber and are absorbed into the headspace.

For investigation of influence of temperature on extraction efficiency, a range of temperature from 40°C to 80°C was investigated. The maximum response was reached when the Temperature was close to 68 and the salt concentration was 10.5 (% w/v).

At a salt concentration > 10.5 (% w/v), the response is decreased. This behaviour can be explained by considering the saturation problems when the salt concentration was higher [38].

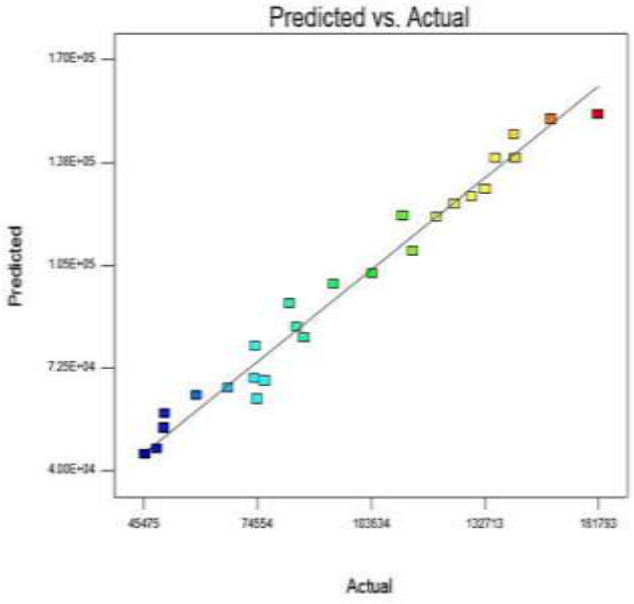

Fig. 7. Predicted vs. actual data for the PAHs.

Also, the effect of extraction time was investigated in rang 5-30 min. As shown in Fig. 7 a, the response increased by increasing the extraction time up to 30 min. The plot of the predicted values of response

versus the actual values is shown in Fig. 8, which demonstrates a good fit.

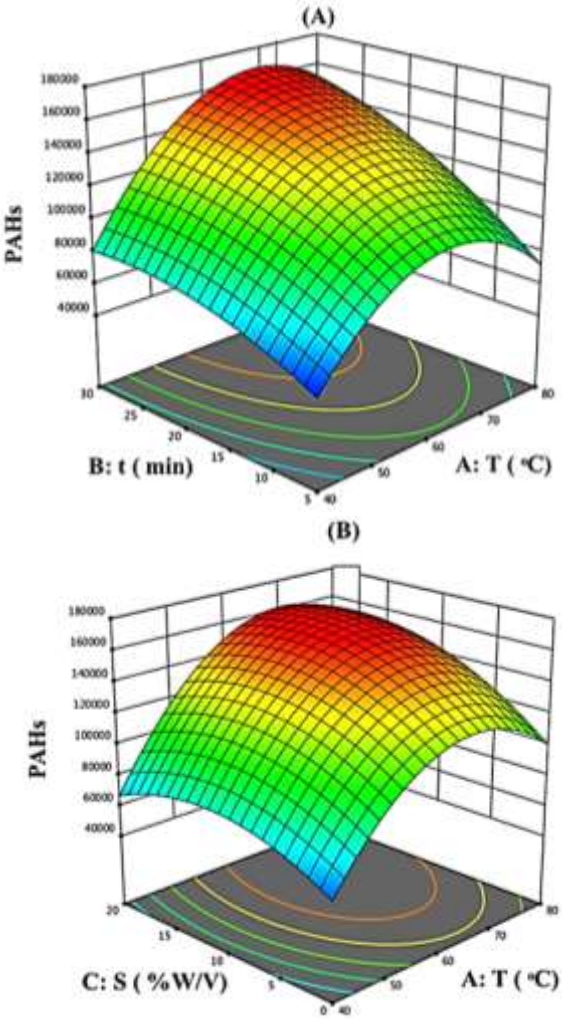

Fig. 8. Response surface for (A) temperature versus time and (B) temperature versus salt mass obtained in the extraction of analytes by HS-SPME.

Fig. 9 shows the normal probability plot for the model residue, which indicates that errors are evenly distributed and supports a least-square fit. Fig. 10 shows the plots of predicted values obtained for the optimization of the microextraction. The predicted optimal values of the independent variables were found to be at an A (T) =70, B (t) = 30, C(S) = 14 and D (R) = 530 to achieve the maximum of response as shown in Fig. 11 with the overall desirability of 1. A desirability value of 1.00 indicates that the estimated function can well represent the experimental model and the desired conditions.

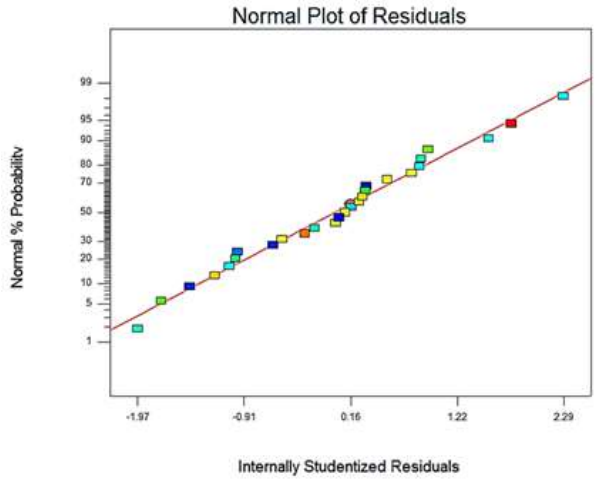

Fig. 9. The normal probability plot for the residuals.

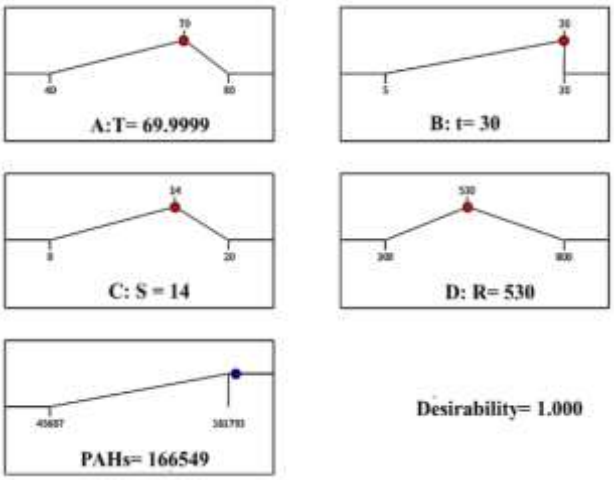

Fig. 10. The desirability profile for the predicted values was obtained for the optimization of the microextraction.

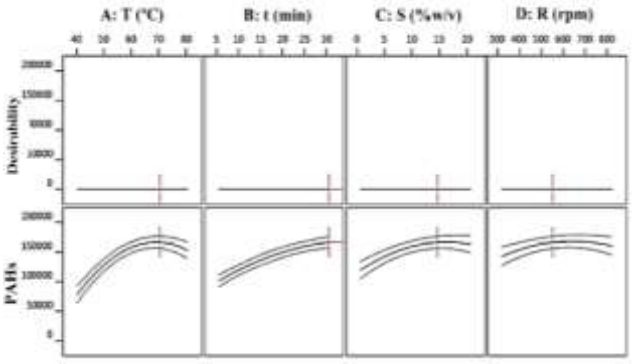

Fig. 11. Profiles for predicted value and desirability function for PAHs.

3.3. Selectivity of prepared fibers

The extraction selectivity of the UMCM-1-DES/MIP fiber were compared for solid phase microextraction of PAHs (1-naphthol, 2-naphthol, anthracene, phenanthrene) by extracting different

compounds including, phenol, pyrene, progesterone and testosterone. Different solutions of the mentioned compounds (concentration: 5 μg L^{-1}) were prepared individually. Fig. 12 shows the peak area of all compounds extracted with the UMCM-1-DES/MIPs and NIP fibers. The peak area of four analytes and comparative compounds with the MIP fibers were significantly higher than those of the NIP fibers. Additionally, it was observed that the extraction yields of the other compounds were lower using MIP than target analytes, which is mainly attributed to the different spatial structures of the comparative compounds from the template, leading to lower extraction efficiency. This indicates that the MIP fibers had greater affinity with the target analyte molecules. This can be attributed to the more suitable binding sites for the target analytes due to an efficient imprinting effect and the difference in size and functional groups type. However, other compounds including progestrone and testestrone as they have no similarity in size, shape and functional groups to anthracene, must have been adsorbed mainly by a non-specific adsorption mechanism.

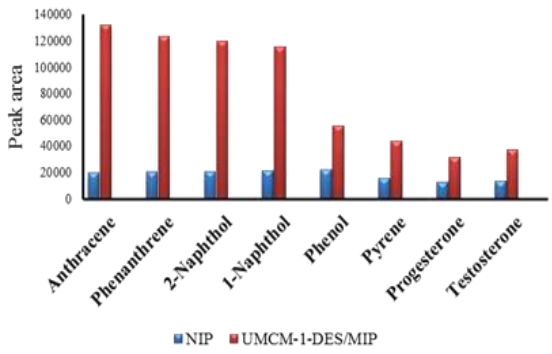

Fig. 12. Comparison of the extraction selectivity of the UMCM-1-DES/MIPs and NIP fibers for target compounds (1-naphthol, 2-naphthol, anthracene, phenantherene) respect to phenol, pyrene, progesterone and testosterone.

3.4. Comparison of the NIP, MIP, UMCM-1/NIP and UMCM-1-*DES/MIP Fibers*

The application of MIP can overcome the drawbacks of absorbents that lack selectivity and affinities for target analytes. To evaluate the efficiency of the UMCM-1-DES/MIP fibers in microextraction of PAHs compounds, four fibers including NIP, MIP, UMCM-1/NIP and UMCM-1-DES/MIP were prepared and were compared. The conditions for preparing these fibers were similar to those explained in Section 2.5. As can be seen in Fig. 13, the UMCM-1-DES/MIP fiber exhibited higher extraction efficiencies than UMCM-1/NIP and MIP fibers, which is due to the simultaneous use of two molecular polymer imprinted and metal-organic

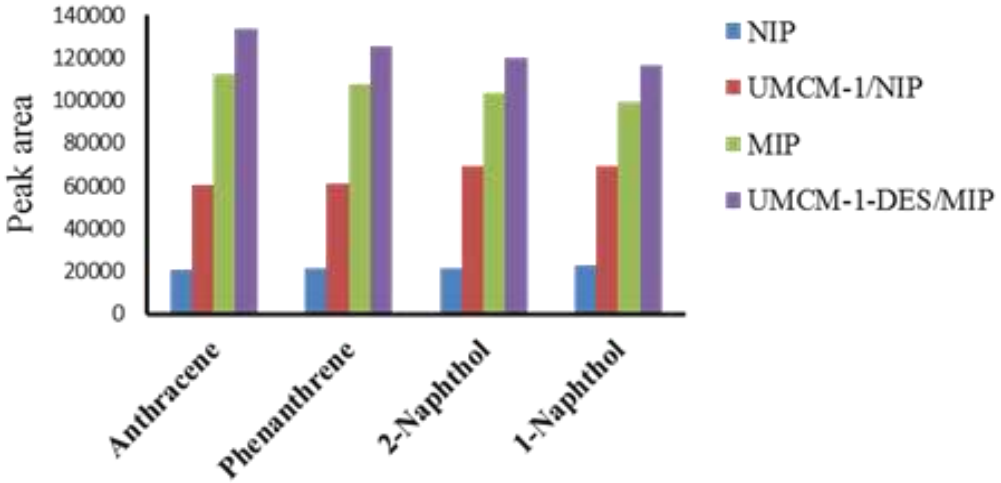

Fig. 13. A comparison of the NIP, MIP, UMCM-1/NIP and UMCM-1-DES/MIP Fibers for the microextraction of PAHs under optimized condition (PAHs concentration: 5 μg L^{-1}).

frameworks, both of which alone have a significant absorption capacity of the target compounds. Additionally, DES as substrate solvent can promote the performance of MOF and MIP and make MIPs more rigidity without shrinking or swelling [21]. The NIPs showed the worst extraction efficiency.

3.5. Method validation

The analytical performance of MOF-DES/MIPs fiber coupled with GC-FID was evaluated under the optimized SPME experimental conditions. The results including linearity (LR), limits of detection (LOD) and limits of quantification (LOQ), enrichment factor, repeatability and accuracy of the method are summarized in Table 4.

By repeating the extraction three times for each concentration level, the linearity (the peak areas versus concentrations) at different concentrations of PAHs standards, were found to be linear in a range of 0.05–150 μgL^{-1} for all compounds with coefficients of determination (R^2) more than 0.996. LOD at S/N of 3 and LOQ at S/N of 10 [39], for ten replicate were between 0.015-0.019 μgL^{-1} and 0.049-0.065 μgL^{-1} respectively. Thus, it shows that the proposed method has low LOD and LOQ, and can be used for microextraction and determining the trace level of target PAHs.

Table 4. Figures of merit of the MOF-DES/MIPs - GC–FID method for determination of PAHs.

Compound	LR (μgL^{-1})	R^2 (μgL^{-1})	LOD (μgL^{-1})	LOQ (μgL^{-1})	EF	RSD[a] (%) (n=5)	
						intra-day	iner-day
Anthracene	0.05– 150	0.997	0.015	0.049	210.5	2.5	3.4
Phenanthrene	0.05– 150	0.997	0.017	0.056	202.3	2.4	3.2
2-Naphthol	0.05– 150	0.996	0.018	0.062	186.2	2.1	3.7
1-Naphthol	0.05– 150	0.996	0.019	0.065	192.7	2.2	3.2

a. Concentration of PAHs = 1 μgL^{-1}

The accuracy of the analytical method was evaluated by calculating the recoveries for the spiked real samples. The extraction recovery (R,%) of PAHs was determined as follows [40]:

$$Recovery\ (\%) = \frac{(C_{found} - C_{unspiked})}{C_{spiked}} \times 100$$

Where C_{found}, $C_{unspiked}$ and C_{spiked} are concentrations of PAHs after addition of known amount of standard in the real samples, concentration of PAHs in real sample, and concentration of known amount of standard added to the real sample, respectively.

To check precision, the intra-day (on the same day) and inter-day (consecutive 5 days) relative standard deviations (RSDs) [41] and accuracies of the current method were evaluated by analyzing samples solutions at three concentration levels. RSD were in a range of 2.0-4.2% and 3.0-4.9% respectively.

To ensure the robustness of the extraction method and for the practicability and preparation of the extraction medium, the repeatability and reproducibility (fiber–fiber) are crucial factors. For this purpose, four fibers were prepared under the same conditions and four replicate extractions were performed for each case. The calculated RSDs (for one fiber) at 5.0 $\mu g\ L^{-1}$ of each analyte were between 1.8% and 2.2% (n = 4) and the RSDs (fiber–fiber) for four individual fibers were between 3.1 and 4.1%. Results in table 5 shows that proposed method has excellent repeatability and reproducibility. In addition, no significant change in the extraction efficiency within 6 months, indicating the high stability of the prepared MOF-DES/MIPs fiber.

The enrichment factors, defined as concentration ratio of PAHs before and after the extraction, were in the range from 186.2 to 210.5.

Table 5. Evaluation of fibers repeatability and reproducibility for the analysis of PAHs using MOF- DES/MIPs - GC–FID.

Compound	RSD (%) (single fiber)[a]	RSD (%) (fiber–fiber)[b]
Anthracene	2.2	3.1
Phenanthrene	2.1	3.4
2-Naphthol	2.1	3.2
1-Naphthol	1.8	4.1

a. Four replicate b. Number of fibers: 4

Considering that the extraction was done in head space mode, the fiber is placed in the headspace of samples and is not in direct contact with the sample matrix, so the fiber is only exposed to volatile and semi volatile compounds, as a result of which the selectivity and lifetime of the fiber increases compared to the direct mode.

3.5.1. Real sample analysis

The SPME–GC method developed with the MOF-DES/MIPs fiber was applied to determination of PAHs in soil, vegetables and different water samples. Relative extraction recovery was determined by spiking three different concentrations (1, 50 and 120 μg L^{-1}) of standards in the sample matrix. The analytical results of three replicate analyses of these samples are summarized in Table 6, 7. The PAHs compounds were not detected in the vegetables and different water samples due to their absence or very low concentration (less than LOQ). In the analysis of real samples, t-test conducted to ensure that the recovery results are free from systematic errors. The results indicates non-significant differences between recoveries and 100%. Fig. 14 a, b presents the chromatograms and peak separation of PAHs in the initial standard solution (10 μg L^{-1}) and unspiked soil sample after microextraction using HS-SPME technique which shows that all compounds were analyzed within 20 minutes.

PAHs relative recovery in the range of 94.3-106.10% with RSDs of below 4.5% confirm the ability of the proposed method as an efficient and credible technique in the analysis of real samples. In addition, the synthesized MOF-DES/MIPs fiber can be reused for more than 20 times.

Table 6. Analytical results for determination of PAHs in soil and vegetables samples (n=3).

Sample	analysts	Unspiked (μgL^{-1})	Recovery[b] of spiked sample (%)		
			1 μgL^{-1}	50 μgL^{-1}	120 μgL^{-1}
Vegetables	Anthracene	ND[a]	98.3 (3.1[b]) (t=0.96[d])	97.3 (3.9) (t=1.23)	99.5 (3.1) (t=0.28)
	Phenanthrene	ND	97.5 (3.7) (t=1.20)	96.3 (4.2) (t=1.58)	95.4 (3.5) (t=2.38)
	2-Naphthol	ND	96.2 (4.3) (t=1.59)	94.7 (4.4) (t=2.20)	94.4 (4.2) (t=2.45)
	1-Naphthol	ND	96.3 (4.1) (t=1.62)	95.6 (4.1) (t=1.94)	95.5 (4.0) (t=2.04)
Soil	Anthracene	1.32	97.6 (3.6) (t=1.18)	98.4 (3.9) (t=0.72)	101.1 (3.3) (t=0.57)
	Phenanthrene	0.65	96.3 (3.1) (t=2.15)	98.5 (4.3) (t=0.61)	97.2 (3.1) (t=1.61)
	2-Naphthol	ND	95.3 (3.3) (t=2.59)	97.8 (3.1) (t=1.26)	98.7 (4.1) (t=0.55)
	1-Naphthol	ND	96.2 (3.1) (t=2.21)	98.1(3.9) (t=0.86)	96.5 (3.9) (t=1.61)

a. ND: Not detected
b. Recovery values are average of three replicates
c. Relative standard deviations of recoveries
d. t_{cal}: calculated t value ($t < t_{cri}$ (2.92) indicates non-significant differences between recoveries and 100%). For one-tailed test, P = 0.05, 2 degrees of freedom, the critical value t is 2.92.

Table 7. Analytical results for determination of PAHs in different water samples (n=3).

Sample	analysts	Unspiked (μgL^{-1})	Recovery [b] of spiked sample (%)		
			1 μgL^{-1}	50 μgL^{-1}	120 μgL^{-1}
Tap water	Anthracene	ND[a]	101.3 (2.1[c]) (t=1.06[d])	102.4 (1.9) (t=2.13)	99.5 (2.3) (t=0.38)
	Phenanthrene	ND	97.3 (1.8) (t=2.67)	98.2 (1.9) (t=1.67)	98.4 (1.6) (t=1.76)
	2-Naphthol	ND	96.8 (2.2) (t=2.60)	97.4 (2.3) (t=2.01)	96.3 (2.8) (t=2.38)
	1-Naphthol	ND	97.4 (2.7) (t=1.71)	96.3 (2.3) (t=2.89)	96.4 (2.8) (t=2.31)
River water	Anthracene	ND	101.5 (2.3) (t=1.11)	103.5 (2.6) (t=2.25)	100.3 (1.7) (t=0.30)
	Phenanthrene	ND	98.6 (2.7) (t=0.90)	97.5 (2.6) (t=1.70)	99.4 (2.8) (t=0.37)
	2-Naphthol	ND	96.7 (2.2) (t=2.68)	97.4 (2.9) (t=1.59)	96.8 (2.9) (t=1.97)
	1-Naphthol	ND	97.1 (2.1) (t=2.46)	96.8 (2.5) (t=2.29)	96.5 (2.3) (t=2.73)
Wastewater	Anthracene	ND	101.8 (4.3) (t=0.71)	104.6 (3.6) (t=2.11)	100.4 (2.1) (t=0.32)
	Phenanthrene	ND	96.5 (2.7) (t=2.32)	96.1 (2.8) (t=2.51)	97.1 (4.2) (t=1.23)
	2-Naphthol	ND	96.2 (2.9) (t=2.35)	95.2 (3.8) (t=2.30)	95.3 (3.0) (t=2.85)
	1-Naphthol	ND	96.1 (2.7) (t=2.60)	95.2 (3.9) (t=2.24)	95.3 (3.0) (t=2.85)
Ground drainage water	Anthracene	ND	102.6 (4.2) (t=1.04)	104.2 (2.9) (t=2.41)	106.1(4.1) (t=2.43)
	Phenanthrene	ND	97.5 (3.2) (t=1.39)	96.5 (2.8) (t=2.24)	97.2 (4.1) (t=1.22)
	2-Naphthol	ND	96.3 (2.6) (t=2.56)	95.4 (4.4) (t=1.90)	96.7 (2.2) (t=2.69)
	1-Naphthol	ND	96.1 (3.1) (t=2.27)	95.4 (3.5) (t=2.39)	95.5 (3.0) (t=2.72)

a. ND: Not detected
b. Recovery values are average of three replicates
c. Relative standard deviations of recoveries
d. t_{cal}: calculated t value ($t < t_{cri}$ (2.92) indicates non-significant differences between recoveries and 100%) For one-tailed test, P = 0.05, 2 degrees of freedom, the critical value t is 2.92.

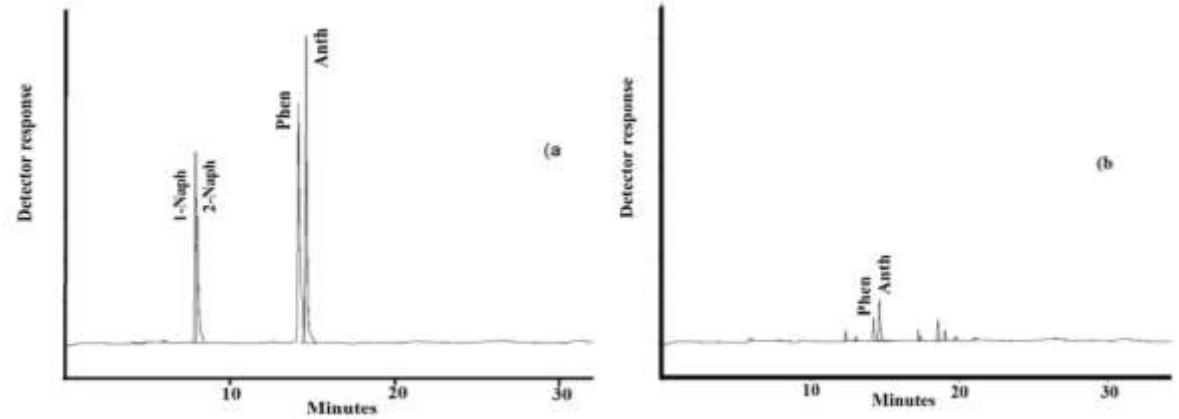

Fig. 14. Chromatograms of (a) standard solution of the PAHs (anthracene, phenanthrene, 1-naphtol and 2-naphtol) (10 µg L^{-1} of each analytes); (b) unspiked soil sample.

3.5.2. Comparison with related works

A comparison of the present work for determination of PAHs with other techniques is presented in Table 8. It can be inferred the current method for analysis of PAHs enhances the sensitivity and efficiency. Also, the developed MOF-DES/MIPs-SPME is an efficient extraction method because of selective adsorption sites for PAHs on the surface of MOF-DES/MIPs fiber. Compared with the reported methods, the MOF-DES/MIPs–SPME technique shows several advantages like good precision, low LODs, wide linear range, short extraction time and less hazardous for the environmental. Also, the utilization of stable hydrophobic DES system as a key factor facilitates the rapid extraction of the PAHs from their matrices to the surface of the fiber, so provides a fast and sustainable sample preparation for the preconcentration of PAHs in complex tissues prior to GC analysis.

Table 8. A comparison between different SPME materials for the determination of PAHs in real samples.

Methods	Material	LDR	LODs (μgL-1)	RSD (%) (μgL-1)	R (%)	Ref.
DI-SPME- GC-FID	Molybdenum oxide	2–600	0.75-1.25	<6.4	81-113	42
DI-SPME- GC-FID	TiO2 nanowires	0.1–200	0.1-3.2 ng/L	4.3-7.3	96-105	43
HS-SPME-GC-FID	Perhydroxy cucurbit uril	0.1–1000	0.03-0.15	1.9-4.7	90-109	44
DI-SPME-GC-FID	Bio-MOF-1	0.1–100	0.02–5.57	2.3–9.3	80-115	45
HS-SPME-GC-MS	MOF-199@GO	0.1–200	0.027–0.041	1.6–2.3	93-103	38
HS-SPME- GC-FID	Graphene	0.05–50	0.01–0.09	4.3–9.8	93-102	46
HS-SPME- GC- FID	Polymeric ionic liquids	0.02–20	0.01-0.04	3.3–7.2	67-130	47
DI-SPME-GC-MS	cork	0.03	0.1- 10	<15.7	70-103	48
DI-SPME-GC-FID	graphene	0.05-200	0.004-0.5	9.3	79-116	49
HS-SPME- GC-FID	MOF- DES/MIPs	0.05-120	0.015-0.019	2.0- 4.9	94-106	This work

All these facts and results indicate that in addition to saving energy and time, higher extraction recoveries can also be achieved by the proposed method.

4. Conclusions

Main objective of the present work was to investigate the potential applications of MOF materials as adsorbent for the SPME of PAHs in soil, vegetables and different water samples. In order to solve the main drawbacks of the MOF, which is weakness in chemical stability in chemical environments, molecular imprinted polymer and Deep Eutectic Solvents (DESs) (as substrate solvent) were used. This can improve the selectivity, kinetics in adsorption and desorption of analytes, analyte positioning target and rate of binding of target compounds in the adsorbent tissue. It is noteworthy that the juxtaposition of MOF, DES and MIP can improves the unique properties such as capacity, selectivity and chemical stability of fibers. The high selectivity is related to the fact that the target fiber is made of a molecular imprinted polymer that can only extract and load template molecules and similar compounds. Under the most favorable conditions, this method provides some operational advantages such as use of low-cost eutectic solvent, simplicity of experimental procedure, particularly good LOD, linearity, and satisfactory repeatability. Overall, this study demonstrated that the developed method is an efficient technique for the SPME of PAHs in the real sample.

5. Acknowledgments

The Authors greatly appreciate the financial support of this work by Shahid Chamran University of Ahvaz, Research Council.

6. References

[1] Martorell, I., Perelló, G., Martí-Cid, R., Castell, V., Llobet, J. M., & Domingo, J. L. (2010). Polycyclic aromatic hydrocarbons (PAH) in foods and estimated PAH intake by the population of Catalonia, Spain: temporal trend. *Environment international*, *36*(5), 424-432.

[2] Sojinu, O. S., Wang, J. Z., Sonibare, O. O., & Zeng, E. Y. (2010). Polycyclic aromatic hydrocarbons in sediments and soils from oil exploration areas of the Niger Delta, Nigeria. *Journal of Hazardous Materials*, *174*(1-3), 641-647.

[3] Fan, C., Cao, X., Han, T., Pei, H., Hu, G., Wang, W., & Qian, C. (2019). Selective microextraction of polycyclic aromatic hydrocarbons using a hydrophobic deep eutectic solvent composed with an iron oxide-based nanoferrofluid. *Microchimica Acta*, *186*, 1-10.

[4] Helalat–Nezhad, Z., Ghanemi, K., & Fallah–Mehrjardi, M. (2015). Dissolution of biological samples in deep eutectic solvents: an approach for extraction of polycyclic aromatic hydrocarbons followed by liquid chromatography-fluorescence detection. *Journal of Chromatography A*, *1394*, 46-53.

[5] Makoś, P., Przyjazny, A., & Boczkaj, G. (2018). Hydrophobic deep eutectic solvents as "green" extraction media for polycyclic aromatic hydrocarbons in aqueous samples. *Journal of Chromatography A*, *1570*, 28-37.

[6] Rahimi, M., Bahar, S., Heydari, R., & Amininasab, S. M. (2019). Determination of quercetin using a molecularly imprinted polymer as solid-phase microextraction sorbent and high-performance liquid chromatography. *Microchemical Journal*, *148*, 433-441.

[7] Amiri, A., Ghaemi, F., & Maleki, B. (2019). Hybrid nanocomposites prepared from a metal-organic framework of type MOF-199 (Cu) and graphene or fullerene as sorbents for dispersive solid phase extraction of polycyclic aromatic hydrocarbons. *Microchimica Acta*, *186*, 1-8.

[8] Chen, X. F., Zang, H., Wang, X., Cheng, J. G., Zhao, R. S., Cheng, C. G., & Lu, X. Q. (2012). Metal–organic framework MIL-53 (Al) as a solid-phase microextraction adsorbent for the determination of 16 polycyclic aromatic hydrocarbons in water samples by gas chromatography–tandem mass spectrometry. *Analyst*, *137*(22), 5411-5419.

[9] Mirzajani, R., Kardani, F., & Ramezani, Z. (2020). Fabrication of UMCM-1 based monolithic and hollow fiber–Metal-organic framework deep eutectic solvents/molecularly imprinted polymers and their use in solid phase microextraction of phthalate esters in yogurt, water and edible oil by GC-FID. *Food chemistry*, *314*, 126179.

[10] Mollahhosseini, A., Abbasi, S. (2018). Polyacrylonitrile electrospun nanofibers as a new coating material for solid-phase microextraction: Application to the preconcentration and determination of phthalates in aqueous samples. Applied Chemistry Today, 13(47), 263-274. (in persion).

[11] Zhang, S., Du, Z., & Li, G. (2011). Layer-by-layer fabrication of chemical-bonded graphene coating for solid-phase microextraction. *Analytical chemistry*, *83*(19), 7531-7541.

[12] Cui, X. Y., Gu, Z. Y., Jiang, D. Q., Li, Y., Wang, H. F., & Yan, X. P. (2009). In situ hydrothermal growth of metal− organic framework 199 films on stainless steel fibers for solid-phase microextraction of gaseous benzene homologues. *Analytical chemistry*, *81*(23), 9771-9777.

[13] Feng, J., Sun, M., Liu, H., Li, J., Liu, X., & Jiang, S. (2010). Au nanoparticles as a novel coating for solid-phase microextraction. *Journal of Chromatography A*, *1217*(52), 8079-8086.

[14] Fu HeYun, F. H., & Zhu DongQiang, Z. D. (2012). In situ hydrothermal grown silicalite-1 coating for solid-phase microextraction.

[15] Mirzajani, R., Kardani, F., & Ramezani, Z. (2019). Preparation and characterization of magnetic metal–organic framework

nanocomposite as solid-phase microextraction fibers coupled with high-performance liquid chromatography for determination of non-steroidal anti-inflammatory drugs in biological fluids and tablet formulation samples. *Microchemical Journal*, *144*, 270-284. [16] Fan, Y. H., Mou, X. X., Qin, S. B., Li, X. S., & Qi, S. H. (2019). Study on four metal organic frameworks as cleanup adsorbents for polycyclic aromatic hydrocarbons determined by GC-MS/MS. *Microchimica Acta*, *186*, 1-9.

[17] Mirzajani, R., Arefiyan, E., (2019). Construction and evaluation of a graphene oxide functionalized aminopropyltriethoxy silane surface molecularly imprinted polymer potentiometric sensor for dipyridamole detection in urine and pharmaceutical samples, *Journal of the Brazilian Chemical Society*, 30 (9), 1874-1886

[18] Mirzajani R., Keshavarz A., (2019). The core–shell nanosized magnetic molecularly imprinted polymers for selective preconcentration and determination of ciprofloxacin in human fluid samples using a vortex-assisted dispersive micro- solid-phase extraction and high- performance liquid chromatography, *Journal of the Iranian Chemical Society*, 16, 2291-2306.

[19] Pourkazem, Sh., Amirzehni, M. (2019). Synthesis of magnetic nanocomposite based on molecularly imprinted polymer and its performance evaluation as adsorbents in the analysis of antibiotic cephalexin. Applied Chemistry Today, 14(52), 321-336. (in persion).

[20] Shirzadmehr, A., Bagheri, H. (2018). Fabrication of potentiometric sensor based on new and high-performance nanocomposite of molecular imprinting for the determination of tramadol. Applied Chemistry Today, 13(47), 197-212. (in persion).

[21] Madikizela, L. M., Ncube, S., Nomngongo, P. N., & Pakade, V. E. (2022). Molecular imprinting with deep eutectic solvents: Synthesis, applications, their significance, and benefits. *Journal of Molecular Liquids*, *362*, 119696.

[22] Mirzajani, R., Karami, S. (2021). Dispersive micro solid phase extraction based on surface magnetic molecular imprinted polymer and deep eutectic solvent with optimization by central composite design for determination of dipyridamole in pharmaceutical and biological samples. Applied Chemistry Today, 16(58), 47-62. (in persion).

[23] Li, G., Ahn, W. S., & Row, K. H. (2016). Hybrid molecularly imprinted polymers modified by deep eutectic solvents and ionic liquids with three templates for the rapid simultaneous purification of rutin, scoparone, and quercetin from Herba Artemisiae Scopariae. *Journal of separation science*, *39*(23), 4465-4473.

[24] Li, G., Wang, X., & Row, K. H. (2017). Magnetic solid-phase extraction with Fe3O4/molecularly imprinted polymers modified by deep eutectic solvents and ionic liquids for the rapid purification of alkaloid isomers (theobromine and theophylline) from green tea. *Molecules*, *22*(7), 1061.

[25] Kardani, F., Mirzajani, R., Tamsilian, Y., & Kiasat, A. (2023). The residual determination of 39 antibiotics in meat and dairy products

using solid-phase microextraction based on deep eutectic solvents@ UMCM-1 metal-organic framework/molecularly imprinted polymers with HPLC-UV. *Food Chemistry Advances*, *2*, 100173.

[26] Kardani, F., Mirzajani, R., & Ramezani, Z. (2018). Direct cholesterol and β-sitosterol analysis in food samples using monolithic molecularly-imprinted solid-phase microextraction fibers coupled with high performance liquid chromatography. *Journal of the Iranian Chemical Society*, *15*, 2877-2888.

[27] Fathi, M., Rajabi, H. R., Khajehsharifi, H., Gorjizadeh, A. (2024). Application of Liquid Phase Microextraction Method Based on Deep Eutectic Solvents for Pre-Concentration and Spectrophotometric Determination of Purpurin Dye. Applied Chemistry Today, 19(70), 135-150. (in persion).

[28] Dai, Y., Van Spronsen, J., Witkamp, G. J., Verpoorte, R., & Choi, Y. H. (2013). Natural deep eutectic solvents as new potential media for green technology. *Analytica chimica acta*, *766*, 61-68. [29] Abbott, A. P., Capper, G., Davies, D. L., McKenzie, K. J., & Obi, S. U. (2006). Solubility of metal oxides in deep eutectic solvents based on choline chloride. *Journal of Chemical & Engineering Data*, *51*(4), 1280-1282.

[30] Gao, Z. T., Li, Z. M., Zhou, Y., Shu, X. J., Xu, Z. H., & Tao, D. J. (2023). Choline chloride plus glycerol deep eutectic solvents as non-aqueous absorbents for the efficient absorption and recovery of HCl gas. *New Journal of Chemistry*, *47*(24), 11498-11504.

[31] Bowen, H., Durrani, R., Delavault, A., Durand, E., Chenyu, J., Yiyang, L., ... & Fei, G. (2022). Application of deep eutectic solvents in protein extraction and purification. *Frontiers in Chemistry*, *10*, 912411.

[32] Ling, J. K. U., & Hadinoto, K. (2022). Deep eutectic solvent as green solvent in extraction of biological macromolecules: A review. *International Journal of Molecular Sciences*, *23*(6), 3381.

[33] Sakti, A. S., Saputri, F. C., & Mun'im, A. (2019). Optimization of choline chloride-glycerol based natural deep eutectic solvent for extraction bioactive substances from Cinnamomum burmannii barks and Caesalpinia sappan heartwoods. *Heliyon*, *5*(12).

[34] Santos, M. D., Cerqueira, M. R., de Oliveira, M. A., Matos, R. C., & Matos, M. A. (2014). Box–Behnken design applied to ultrasound-assisted extraction for the determination of polycyclic aromatic hydrocarbons in river sediments by gas chromatography/mass spectrometry. *Analytical methods*, *6*(6), 1650-1656.

[35] Patil, D. V., Rallapalli, P. B. S., Dangi, G. P., Tayade, R. J., Somani, R. S., & Bajaj, H. C. (2011). MIL-53 (Al): an efficient adsorbent for the removal of nitrobenzene from aqueous solutions. *Industrial & engineering chemistry research*, *50*(18), 10516-10524.

[36] Ullah, S., Bustam, M. A., Assiri, M. A., Al-Sehemi, A. G., Gonfa, G., Mukhtar, A., ... & Mellon, N. B. (2020). Synthesis and characterization of mesoporous MOF UMCM-1 for CO2/CH4 adsorption; an experimental, isotherm modeling and thermodynamic

study. *Microporous and Mesoporous Materials*, *294*, 109844.

[37] Zhou, Q., & Gao, Y. (2014). Determination of polycyclic aromatic hydrocarbons in water samples by temperature-controlled ionic liquid dispersive liquid–liquid microextraction combined with high performance liquid chromatography. *Analytical methods*, *6*(8), 2553-2559.

[38] Kardani, F., Mirzajani, R., & Ramezani, Z. (2019). Determination of nanomolar dissolved polycyclic aromatic hydrocarbons in different water and wastewater samples using a metal-organic framework-199@ graphene oxide fiber and headspace solid-phase microextraction. *Desalination and Water Treatment*, *144*, 99-115.

[39] Safavi, A., Mirzajani, R., (2002). Catalytic determination of traces of silver (I) using the oxidation of Janus green with peroxodisulfate, *Analytical Sciences,* 18 (3), 329-332.

[40] Mirzajani, R., Kardani, F., Ramezani, Z., (2021). The fabrication of a novel polyacrylonitrile/reduced graphene oxide-amino-halloysite/bimetallic metal–organic framework electrospun nanofiber adsorbent for the ultrasonic-assisted thin-film microextraction of fatty acid methyl esters in dairy products with gas chromatography-flame ionization detection, *RSC.Advances*. 11**,** 14686-14699

[41] Mirzajani, R., Bavarsadian Kha, J., (2024) Electrospun nanofiber composite based on bimetallic metal–organic framework/halloysite nanotubes/deep eutectic solvents/molecularly imprinted polymers for thin film microextraction of sulfonamides in milk, eggs and chicken meat by HPLC analysis, *Microchemical. Journal*, 23, 110950

[42] Liu, H., Wang, X., Fan, H., & Dang, S. (2019). Durable molybdenum oxide coated solid-phase microextraction fiber for highly selective and efficient extraction of polycyclic aromatic hydrocarbons in water. *Journal of separation science*, *42*(10), 1878-1885.

[43] Zhang, R., Wang, Z., Wang, Z., Wang, X., & Du, X. (2019). Tailoring the selectivity of titania nanowire arrays grown on titanium fibers by self-assembled modification of trichlorophenylsilane for solid-phase microextraction of polycyclic aromatic hydrocarbons. *Microchimica Acta*, *186*, 1-9.

[44] Dong, N., Li, T., Luo, Y., Shao, L., Tao, Z., & Zhu, C. (2016). A solid-phase microextraction coating of sol–gel-derived perhydroxy cucurbit [6] uril and its application on to the determination of polycyclic aromatic hydrocarbon. *Journal of Chromatography A*, *1470*, 9-18.

[45] Huo, S. H., Yu, J., Fu, Y. Y., & Zhou, P. X. (2016). In situ hydrothermal growth of a dual-ligand metal–organic framework film on a stainless steel fiber for solid-phase microextraction of polycyclic aromatic hydrocarbons in environmental water samples. *RSC advances*, *6*(17), 14042-14048.

[46] Zakerian, R., & Bahar, S. (2019). Electrochemical exfoliation of pencil graphite for preparation of graphene coating as a new versatile SPME fiber for determination of polycyclic aromatic hydrocarbons by gas chromatography. *Microchimica Acta*, *186*, 1-7.

[47] Merdivan, M., Pino, V., & Anderson, J. L. (2017). Determination of volatile polycyclic

aromatic hydrocarbons in waters using headspace solid-phase microextraction with a benzyl-functionalized crosslinked polymeric ionic liquid coating. *Environmental technology*, *38*(15), 1897-1904.

[48] Dias, A. N., Simão, V., Merib, J., & Carasek, E. (2013). Cork as a new (green) coating for solid-phase microextraction: determination of polycyclic aromatic hydrocarbons in water samples by gas chromatography–mass spectrometry. *Analytica chimica acta*, *772*, 33-39.

[49] Fan, J., Dong, Z., Qi, M., Fu, R., & Qu, L. (2013). Monolithic graphene fibers for solid-phase microextraction. *Journal of Chromatography A*, *1320*, 27-32.